Received: 25 August 2019 | Revised: 27 September 2019 | Accepted: 2 October 2019

DOI: 10.1002/cne.24788

RESEARCH ARTICLE

JCN RESEARCH IN SYSTEMS NEUROSCIENCE THE JOURNAL OF COMPARATIVE NEUROLOGY WILEY

The reniform body: An integrative lateral protocerebral neuropil complex of Eumalacostraca identified in Stomatopoda and Brachyura

Hanne Halkinrud Thoen[1] | Gabriella Hannah Wolff[2] | Justin Marshall[1] | Marcel E. Sayre[3] | Nicholas James Strausfeld[4]

[1]Sensory Neurobiology Group, Queensland Brain Institute, University of Queensland, Brisbane, Australia

[2]Department of Biology, University of Washington, Seattle, Washington

[3]Lund Vision Group, Department of Biology, Lund University, Lund, Sweden

[4]Department of Neuroscience, School of Mind, Brain and Behavior, University of Arizona, Tucson, Arizona

Correspondence
Nicholas James Strausfeld, Department of Neuroscience, School of Mind, Brain and Behavior, University of Arizona, Tucson, AR.
Email: flybrain@neurobio.arizona.edu

Funding information
Asian Office of Aerospace Research and Development, Grant/Award Number: 12-4063; Australian Research Council, Grant/Award Number: FL140100197; National Science Foundation, Grant/Award Number: 11754798; Lizard Island Research Station; Lizard Island Research Foundation; University of Arizona Regents Fund; University of Arizona's Center for Insect Science

Abstract

Mantis shrimps (Stomatopoda) possess in common with other crustaceans, and with Hexapoda, specific neuroanatomical attributes of the protocerebrum, the most anterior part of the arthropod brain. These attributes include assemblages of interconnected centers called the central body complex and in the lateral protocerebra, situated in the eyestalks, paired mushroom bodies. The phenotypic homologues of these centers across Panarthropoda support the view that ancestral integrative circuits crucial to action selection and memory have persisted since the early Cambrian or late Ediacaran. However, the discovery of another prominent integrative neuropil in the stomatopod lateral protocerebrum raises the question whether it is unique to Stomatopoda or at least most developed in this lineage, which may have originated in the upper Ordovician or early Devonian. Here, we describe the neuroanatomical structure of this center, called the reniform body. Using confocal microscopy and classical silver staining, we demonstrate that the reniform body receives inputs from multiple sources, including the optic lobe's lobula. Although the mushroom body also receives projections from the lobula, it is entirely distinct from the reniform body, albeit connected to it by discrete tracts. We discuss the implications of their coexistence in Stomatopoda, the occurrence of the reniform body in another eumalacostracan lineage and what this may mean for our understanding of brain functionality in Pancrustacea.

KEYWORDS

brain, Eumalacostraca, evolution, homology, RRID AB_ 477019, RRID AB_1157911, RRID AB_301787, RRID AB_528479, RRID AB_572263, RRID AB_572268, sensory integration

1 | INTRODUCTION

Before his untimely death at 33 years of age, the Italian biologist Giuseppe Bellonci (1855–1888) was already recognized by his peers as an unusually explorative comparative neuroanatomist (Facchini, 1890). His publications covered vertebrate embryology, the representation of the eye in the brain, considerations of consciousness, as well as comparative studies of olfactory pathways across crustaceans, insects, and vertebrates in which he explored the functional and historical significance of corresponding neural architectures. Among his monographs, there is one that exemplifies both the apogee of neuroanatomical analysis of his day, before the advent of reduced silver methods, and his fascination with neural centers that appeared to exist across different animal groups. This is his 1882 monograph describing the optic lobes and their proximal centers in the mantis shrimp *Squilla mantis*, which we draw from here to begin our description (Figure 1a, b). In his monograph, Bellonci identifies two continuous centers, the corpo emielissoidale and corpo allungato, which he said were identical to, respectively, the calyx

and columnar lobes of the insect mushroom body. The monograph also identifies a prominent kidney-shaped center that Bellonci named the corpo reniforme (Eng. "reniform body").

In a recent study by us using an extensive palette of neuroanatomical methods, we confirmed Bellonci's identification of the mushroom body and also identified 13 morphological traits that provide evidence for its phenotypic homology with the like-named center in insects (Wolff, Thoen, Marshall, Sayre, & Strausfeld, 2017). The study by Wolff et al. (2017) also provides a brief description of the stomatopod reniform body, comparing it to an identical center in the varunid shore crab, *Hemigrapsus nudus*. Other studies carried out by the same authors (Thoen, Sayre, Marshall, & Strausfeld, 2018; Thoen, Marshall, Wolff, & Strausfeld, 2017; Thoen, Strausfeld, & Marshall, 2017) show the stomatopods to have elaborate optic lobes and central complex neuropils, most likely due to the high processing demands of their visual system, which has been shown to detect 12 different color channels as well as both linearly and circularly polarized light (Chiou et al., 2008; Cronin & Marshall, 1989; Marshall, 1988; Marshall, Cronin, & Kleinlogel, 2007).

Bellonci used the procedure of fixing neural tissue in osmium vapor, an extremely hazardous method but one providing exquisite anatomical details after the brain is sectioned (Figure 1). It enabled Bellonci to identify major tracts extending to (or from—their polarity was not ascertained) the reniform body. The three most prominent, due to their size and density of their fibers, were called the "reniform body pedunculi," all of which appear to extend to or from unidentified

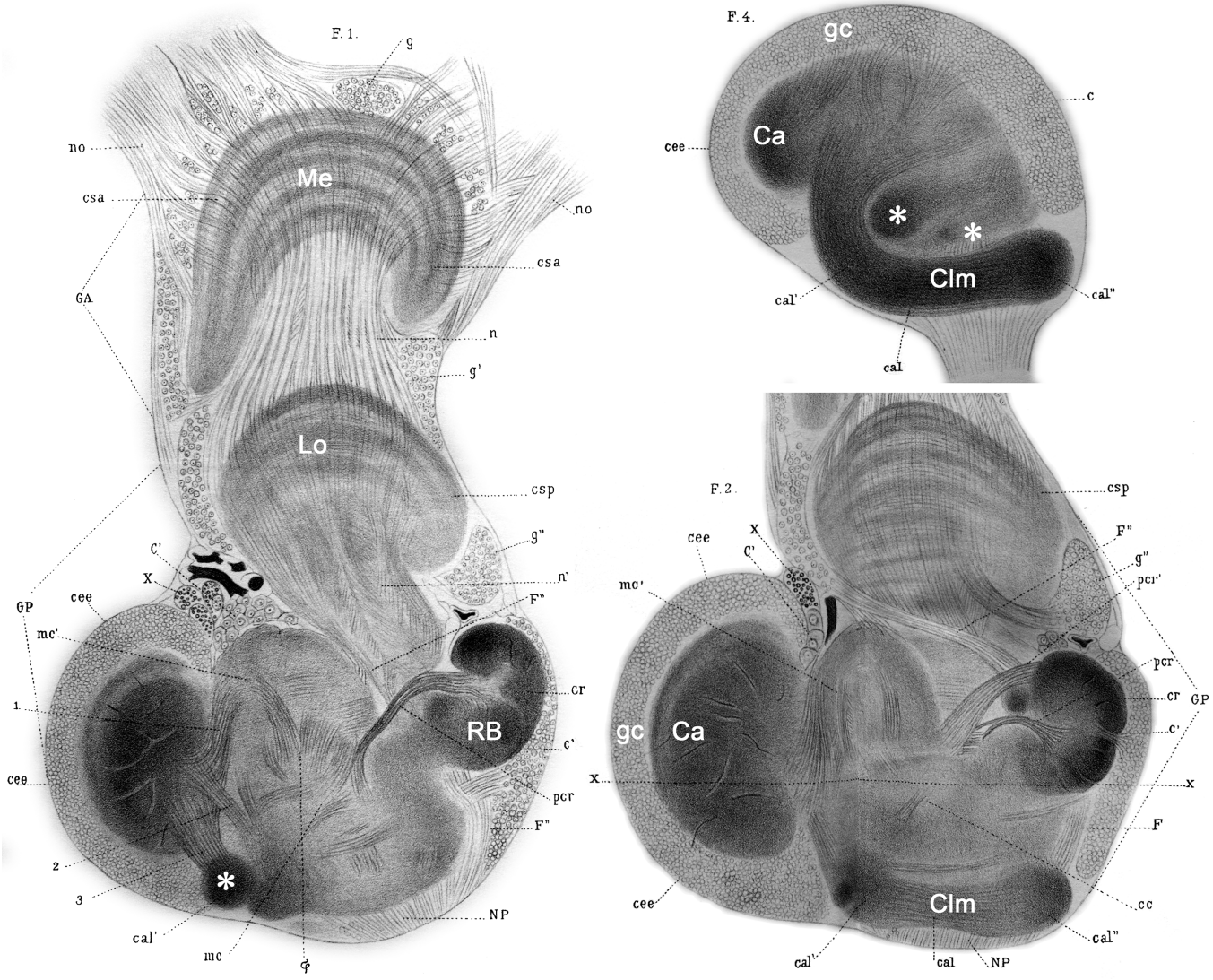

FIGURE 1 Reproduction of Figures 1, 2, and 4 from Bellonci (1882) showing in his F.1 the right lateral protocerebrum of *Squilla mantis* with the optic lobe's medulla (Me) and lobula (Lo) and again at a more superficial level in F.2. Rostral is to the left, distal is upward. Abbreviations are their original size and are not explained. Abbreviations pertaining to the present description, and using modern terminology, have been placed on relevant centers. In F.1, the reniform body (RB) is shown with its large kidney-shaped ensemble of neuropil on the caudal side of the lateral protocerebrum, whereas the mushroom body calyx (Ca), also shown in F.2, bulges out from the rostral side. F.2 shows the largest column of the mushroom body (Clm). The drawing in F.4 is from another preparation, which shows the characteristic shape of the mushroom body: its calyx is shown covered by globuli cell bodies (gc) and giving rise to three columns, one large (Clm) accompanied by two smaller columns (asterisks). Bellonci's own abbreviations refer to fiber tracts, aggregates of cell bodies and various other features

neuropils in the lateral protocerebrum (Figure 1). Other tracts are shown extending to the reniform body from either the medulla or the lobula, the two inner retinotopic neuropils of the optic lobe (Figure 1). Also depicted by Bellonci was the clear division of the reniform body into gyrus-like domains flanked by sulcus-like fissures, which we here show correspond to structures resolved by affinity of the reniform body to antibodies raised against DC0, the catalytic subunit of protein kinase A, required for effective learning and memory by the mushroom bodies of *Drosophila melanogaster* (Skoulakis, Kalderon, & Davis, 1993).

In the final passage of his 1882 monograph, Bellonci compares the lateral protocerebrum of *S. mantis* with the equivalent region in the Mediterranean Sea slater *Sphaeroma serratum*, noting its apparently reduced mushroom body and the complete absence of a reniform body. In asking whether the reniform body occurs generally in malacostracans, Bellonci posed a crucial question that only now assumes importance due to the identification in several decapod lineages of centers that may correspond to the stomatopod mushroom body.

The caridean *Lebbeus groenlandicus*, which is equipped with an insect-like mushroom body (Sayre & Strausfeld, 2019), possesses paired centers, the Bodian-stained neuropils of which morphologically correspond to the stomatopod reniform bodies, as do similar centers in some reptantian decapods equipped with lobed mushroom bodies, such as the marine hermit crab *Pagurus hirsutiusculus* (Strausfeld & Sayre, 2019). As recognized by Hanström (1931), many other reptantians have highly modified centers that lack columnar lobes, which he nevertheless recognized as mushroom bodies but referred to as "hemiellipsoid bodies." Those species also show evidence of reniform bodies (Strausfeld & Sayre, 2019). Observations of Varunidae and Ocypodidae (fiddler crabs), which belong to Brachyura, the evolutionarily youngest reptantian clade (Wolfe et al., 2019), verified they also possess centers corresponding to the stomatopod reniform body. In the varunid crab *Neohelice granulata*, this center is of particular interest because of evidence that it participates in learning and memory, expressed as long-term habituation to noxious visual stimuli (Maza, Sztarker, Shkedy, Peszano, Locatelli, & Delorenzi, 2016).

As well as its individual connections to the visual system, we show that the stomatopod reniform body also sends inputs to the mushroom body calyces, a feature reminiscent of calycal inputs that in insects originate from the lateral horn, a center that flanks the mushroom body distally and which we discuss as a possible reniform body homologue. Finally, we provide further data on reniform body morphology and its sensitivity to anti-DC0 labelling in the shore crab *H. nudus*.

2 | MATERIALS AND METHODS

2.1 | Crustacean species

Species used for this study were mainly *Neogonodactylus oerstedii* (*n* = 50), *Gonodactylus smithii* (*n* = 47), and two *G. chiragra*. *Neogonodactylus* specimens were obtained commercially from the waters off the coast of Florida. *Gonodactylus* were collected off the coast of Lizard Island Research Station, Queensland, Australia (GBRMPA Permit No. G12/35005.1, Fisheries Act No. 140763). The animals were maintained in the laboratory in small, perforated plastic containers in aerated artificial seawater. They were used as soon as possible after collection. Live shore crabs (*H. nudus n* = 40) were collected from designated sites affiliated with the University of Washington's Friday Harbor Marine Biology Laboratories.

2.2 | Texas red fills of tracts and neurons

To identify neuronal pathways projecting to and from the reniform body, mass fills of neurons were carried out according to the method of Ehmer and Gronenberg (2002). Crystals of dextran conjugated with Texas red (3,000 MW #D-3328, ThermoFisher Scientific, Waltham, MA) were made into a paste by placing a speck of dye powder on a glass slide resting on crushed ice and then mixing the dye with the condensing water. A minute droplet of paste was applied to the tip of a glass electrode. An animal cooled to immobility on ice had a window cut into the underside of its eyestalk cuticle allowing direct observation of the lateral protocerebrum and its reniform body and lobula. Then, under binocular microscope observation, the electrode was manually inserted either into the lobula or into the reniform body, left there for 2–3 s, and then withdrawn; the piece of cuticle that was cut off was placed back over the lateral protocerebrum and the hemolymph was allowed to coagulate. This kept the cuticle in place and sealed off the eyestalk. The animal was kept alive submerged in sea water and allowed to move freely for 6–8 hr to allow the transport of the dye through neurons. The stomatopod was then again cooled, its nervous tissue dissected free from the surrounding exoskeleton and muscle to be placed in cold (4°C) 4% paraformaldehyde in 0.1 M phosphate-buffered saline (PBS) overnight. Tissue was next washed in PBS for 5 × 20 min and then dehydrated in an ascending series of ethanol (50, 70, 80, 90, 95, and 100%) for 15 min at each concentration. Tissue was next cleared in a solution of 1:1 methyl salicylate:100% ethanol for 15 min, before being placed in 100% methyl salicylate for at least 1 hr. After the tissue was cleared, it was mounted in Permount (Fisher Chemical, Waltham, MA, SP15-100) using plastic spacer rings to prevent compression and examined using the confocal microscope.

2.3 | Golgi impregnations

Stochastic silver impregnations were carried out using a variation of the mixed Colonnier-rapid technique as described in Li and Strausfeld (1997). Animals were cooled to immobility and decapitated, with the head region immediately being submerged in cold chromation solution (2.5% potassium dichromate with 12% sucrose). Raptorial appendages and antennae pairs A1 and A2 were cut off and slits were cut around the edge of the cornea to facilitate the penetration of fixative. Cuticle and muscle tissue were removed and the tissue was placed in fresh cold chromation solution (1 part

25% glutaraldehyde and 5 parts 2.5% potassium dichromate with 12% sucrose) for 4 days. The tissue was gently washed several times in fresh 2.5% potassium dichromate and placed in a cold solution of 99 parts 2.5% potassium dichromate and 1 part 1% osmium tetroxide. After a further 3 days, the tissue was dipped in distilled water before being placed in 0.75% silver nitrate for 3 days. The last two steps were then repeated for 24 hr each. The tissue was then dehydrated, embedded in Durcupan ACM plastic (Sigma-Aldrich, St. Louis, MO, Cat# 44610; St. Louis, MO) and sectioned at 40 μm using a sliding microtome. Golgi observations used 15 specimens of *G. smithii*, 30 of *N. oerstedii*, and 25 of *H. nudus*.

2.4 | Bodian silver staining

Neuropils were resolved using Bodian's reduced silver stain method (see Bodian, 1936) on 4–8 specimens of each of the species discussed. After fixation of the eyestalks in acetic acid-alcohol-formalin (10 ml 16% paraformaldehyde, 2.5 ml glacial acetic acid, 42 ml 80% ethanol) for 3 hr at room temperature. Tissue was rinsed twice in 50% ethanol, transferred through an ethanol series of 70, 90%, and two changes of 100% ethanol for 10 min each and then soaked in α-terpineol (Sigma-Aldrich; Cat# 432628) for 15 min before being immersed in xylol for an additional 15 min. Tissue was then embedded in paraffin, sectioned at 12 μm, dewaxed and stained.

2.5 | Antibodies

Visualization of neural architectures of lateral protocerebral neuropils was achieved using antibodies listed in Table 1. An antibody against DC0 recognizing the catalytic subunit of protein kinase A in *D. melanogaster* (Skoulakis et al., 1993) preferentially reveals the columnar lobes of stomatopod mushroom bodies and the reniform body (Wolff et al., 2017). Western blot assays of DC0 antibodies used on representatives of Panarthropoda reveal a band around 40 kDa, indicating cross-phyletic specificity of this antibody (Stemme, Iliffe, & Bicker, 2016; Wolff & Strausfeld, 2015). Antibodies against serotonin (anti-5HT, Immunostar. Hudson, WI), glutamic acid decarboxylase (anti-GAD, Sigma-Aldrich, St Louis, MO), and tyrosine hydroxylase (anti-TH, Immunostar, Hudson, WI) were used to distinguish overall cytoarchitectures and neuropil boundaries. Antibodies raised against 5HT have been used for neuroanatomical studies across Arthropoda (Antonsen & Paul, 2001; Harzsch & Hansson, 2008; Nässel, 1988; Wolf & Harzsch, 2012). Anti-GAD and anti-TH detect the enzymatic precursors of gamma-aminobutyric acid (GABA) and dopamine, respectively, and do not require alternative fixation methods, making them compatible with synapsin and α-tubulin labelling. Comparisons of anti-GAD and anti-TH immunolabeling with that of their respective derivatives demonstrate that they, respectively, label putative GABAergic and dopaminergic neurons (Cournil, Helluy, & Beltz, 1994; Crisp, Klukas, Gilchrist, Nartey, & Mesce, 2001; Stemme et al., 2016; Stern, 2009).

2.6 | Neuropil immunohistochemistry

The methods described here are those used in two recent studies on the eumalacostracan brain (Sayre & Strausfeld, 2019; Wolff et al., 2017). About four to eight examples of each species were used for each of the applications using the described antibody combinations. Eyestalk neuropils from 6 *H. nudus* and 12 *N. oerstedii* were used for anti-DC0 immunohistology. Animals were anesthetized to immobility using ice. Eyestalks were removed. Some of the retinal surface was removed to aid fixation before the eyestalks were immersed in ice-cold fixative containing 4% paraformaldehyde in 0.1 M PBS with 3% sucrose (pH 7.4). Within 24 hr, the lateral protocerebrum and attached optic lobes were dissected out and desheathed and left to further fix overnight at 4°C. Neural tissue was then rinsed twice in PBS and then transferred to the embedding medium consisting of 5% agarose and 7% gelatin, where it was left for 30–60 min at 60°C. After cooling to room temperature in plastic molds, the solidified gelatin blocks containing tissue were removed from the molds and post-fixed in 4% paraformaldehyde in PBS for 1 hr at 4°C. Blocks were rinsed twice in PBS and sectioned at 60 μm using a vibratome (Leica VT1000 S, Leica Biosystem, Nussloch, Germany). Sections were washed for 2 × 20 min in PBS containing 0.5% Triton-X (PBST). Tissue was then blocked for 1 hr in PBST with 0.5% normal donkey serum (NDS; Jackson ImmunoResearch; RRID: AB_2337258) before primary antibody incubation at the dilutions listed in Table 1. Sections were left to incubate overnight on a rotator at room temperature. The next morning, sections were rinsed in PBST six times during 1 hr. Donkey anti-mouse Cy3 and donkey anti-rabbit Cy5 or Alexa 647 (Jackson ImmunoResearch; RRID: AB_2340813; RRID: AB_2340607; RRID: AB_2492288, respectively) IgG secondary antibodies were added to Eppendorf tubes at a concentration of 1:400 and spun for 12 min at 11,000*g*. The top 900 μl of the secondary antibody solution was added to the tissue sections, which were then incubated overnight at room temperature on a rotator. To label cell bodies, tissue sections were rinsed twice in 0.1 M Tris–HCl buffer (pH 7.4) and soaked for 1 hr in Tris–HCl buffer containing 1:2,000 of the nuclear stain, Syto13 (ThermoFisher Scientific; Cat# S7575) on a rotator. Sections were then rinsed six times in Tris–HCl during 1 hr and mounted on slides in a medium containing 25% Mowiol (Sigma-Aldrich; Cat# 81381) and 25% glycerol in PBS. Slides were covered using #1.5 coverslips (Fisher Scientific; Cat# 12-544E). The edges of the coverslips were sealed using transparent nail varnish. Slides were stored in flat cardboard slide trays at 4°C. For verification of secondary antibody specificity, primary antibodies were omitted, resulting in complete abolishment of immunolabeling. Alpha-tubulin and synapsin antibodies were used often in conjunction with other primary antibodies, to visualize general neural trajectories, identify neuropils, and resolve their cytoarchitecture. Both antibodies have been widely used across distantly related phyla, suggesting that their respective epitope sites are highly conserved (Andrew, Brown, & Strausfeld, 2012; Brauchle, Kiontke, MacMenamin, Fitch, & Piano, 2009; Harzsch, Anger, & Dawirs, 1997; Klagges et al., 1996; Thazhath, Liu, & Gaertig, 2002).

Anti-TH immunolabeling used a modified staining procedure with shorter fixation and antibody incubation on whole unsectioned tissue. Neural tissue was dissected and fixed in 4% paraformaldehyde in PBS containing 3% sucrose for 30–45 min. Following fixation, tissue was rinsed twice in PBS, and twice in 0.5% PBST during 40 min. Tissue was then transferred to blocking buffer containing 5% NDS in 1% PBST and soaked for 3 hr. The primary antibody against TH was next added to the blocking buffer at a concentration of 1:250. To assist antibody permeation, whole tissues were microwave-treated for two cycles of 2 min on low power (~80 W) followed by a 2 min cooling period (no power) under constant vacuum. Tissue was subsequently left to incubate in primary antibody solution for 2–3 days and was microwave-treated each day.

After primary antibody incubation, tissue was washed with 0.5% PBST six times over the course of 2 hr and then transferred to a solution containing 1:400 Cy3 secondary antibody. Whole mounts were left in secondary antibody overnight on a shaker set at low intensity before being sectioned and mounted as described above. In dual labelling experiments, sectioned tissue labeled with anti-TH was then stained with an additional primary and secondary antibody, also as described above.

2.7 | Synapsin whole mounts

Intact lateral protocerebral neuropils were imaged using confocal microscopy after being treated with an antibody against synapsin I (SYNORF1) kindly deposited with the Developmental Studies Hybridoma Bank (DSHB) by Eric Buchner, DSHB Hybridoma Product 3C11 (see Thoen et al. 2017). Animals were cooled to immobility. The eyestalks were cut off and small slits were cut along the cornea to facilitate the penetration of fixative (4% paraformaldehyde in 0.1 M PBS, pH 7.4), and the rest of the body was disposed of according to regulations. The eyestalks were placed in the fixative (at 4°C) for 2 hr before dissecting out nervous tissue, which was placed in fresh fixative and left overnight. Tissue was next washed in 0.1 M PBS with 0.2% Triton X-100 for 6 × 10 min before pre-incubation for 3 hr in 0.1 M PBS with 0.2% Triton X-100 and 2% normal goat serum (NGS, Life-Technologies, Carlsbad, CA, 50-062Z) at room temperature. The tissue was incubated in a dilution of 1:50 SYNORF1 in 0.1 M PBS with 0.2% Triton X-100 and 2% NGS, and left in the 4°C refrigerator for 6 days. Afterward, tissue was washed in 0.1 M PBS for 5 × 20 min and incubated in Alexa Fluor 647 goat anti-mouse (1:250, Molecular Probes, Eugene, OR, A21236) in 0.1 M PBS with 1% NGS for another 4 days. Finally, the tissue was washed for 3 × 20 min in 0.1 M PBS before being dehydrated in ascending alcohol series, cleared using methyl salicylate and mounted in Permount with spacer rings.

2.8 | Imaging

Confocal images were collected using a Zeiss Pascal 5, a Zeiss 710 or a LSM880 confocal microscope (Zeiss; Jena, Germany). Three-dimensional image projections were made using FIJI (zproject plugin; Schindelin et al., 2012). Brightness, contrast, and color intensity were adjusted using Adobe Photoshop CC (Adobe Systems; San Jose, CA), employing the camera raw filter plugin for initial dehazing and intensity adjustment. Light microscopy images were obtained using a Leitz Orthoplan microscope equipped with PlanApochromat oil-immersion objectives (×40, ×60, and ×100). Series of step-focused image sections (0.5–1.0 μm increments) were stitched together and reconstructed using Helicon Focus (Helicon Soft; Kharkov, Ukraine) or employing the darkening function on Photoshop layering.

TABLE 1 Primary antibodies used in this study

Antibody	Concentration	Host	Immunogen	Supplier; catalogue #; RRID
α-Tubulin	1:100	Mouse (monoclonal)	α-Tubulin derived from the pellicles of the protozoan *Tetrahymena*	DHSB; 12G10; AB_1157911
α-Tubulin	1:250	Rabbit (polyclonal)	Synthetic peptide within human α-tubulin; amino acid 400 to the c-terminus	Abcam (Cambridge, UK); ab15246; AB_301787
Synapsin (SYNORF1)	1:50	Mouse (monoclonal)	*Drosophila* glutathione S-transferase fusion protein	DHSB; 3C11; AB_528479
Serotonin (5HT)	1:1,000	Rabbit (polyclonal)	Serotonin coupled to bovine serum albumin with paraformaldehyde	ImmunoStar; 20080; AB_572263
Glutamic acid decarboxylase (GAD)	1:500	Rabbit (polyclonal)	C-terminus of both the 65- and 67-kDa isoforms of human GAD	Sigma-Aldrich; G5163; AB_ 477019
Tyrosine hydroxylase (TH)	1:250	Mouse (monoclonal)	TH purified from rat PC12 cells	ImmunoStar; 22941; AB_572268
DC0	1:400	Rabbit (polyclonal)	Catalytic subunit of *Drosophila* protein kinase A	Generous gift from Dr. Daniel Kalderon

3 | TERMINOLOGY

The reniform body contains many shrub-like terminals, the branchlets of which end as short ovoid configurations, each comprising tightly packed varicose or spiny processes enclosing swollen terminals or finer processes belonging to other neurons. These composite structures have two size variants: the smaller are referred to here as synaptic pockets; the larger, as synaptic baskets. Both terms are introduced so as to avoid using "microglomerulus," a term commonly used to refer to smaller synaptic complexes in the mushroom body calyx, or "glomeruli," a term used to define elaborate multineuronal subunits of the olfactory lobes.

Descriptions of the orientation and relative positions of neuropils, tracts and cell body clusters refer to the rostro-caudal and proximal-distal neuraxes. Allowing for the extension of the lateral protocerebrum into the eyestalks, these provide identical reference points for describing components of the stomatopod brain or the brains of other pancrustaceans, including insects (Figure S1).

4 | RESULTS

4.1 | Reniform body neuroarchitecture

Three figures from Bellonci's 1882 monograph on *S. mantis* are so accurate as to serve here as an introduction to the general disposition of the two inner optic neuropils (the medulla and lobula) and the lateral protocerebrum proximal to them (Figure 1). The lateral protocerebrum is, as its name suggests, an outgrowth from the brain that, in all malacostracans possessing eyestalks, is situated either in the last segment of the eyestalk (as in stomatopods and in most decapods), or at its base as in land hermit crabs. As shown by Bellonci, the lateral protocerebrum is dominated by three prominent neuropils: the reniform body and the two neuropils that together comprise the mushroom body calyces and their columns (Wolff et al., 2017). Notably, although both the reniform body and mushroom body derive from cell bodies covering the most rostral surface of the lateral protocerebrum, the largest integrative neuropils of these two centers are on opposite sides. With regard to the brain's neuraxis, the mushroom body calyces are rostral, capping the lateral protocerebrum, whereas the main volume of the reniform body is located caudally, almost touching the lower margin of the optic lobe's lobula.

Immunohistological studies of *N. oerstedii* sectioned at a level ventral to its mushroom body calyces (Figure 2a) demonstrate an organization corresponding to that of *S. mantis* or *G. smithii*, or indeed other investigated stomatopod species. As shown in Figure 2a, the optic lobe's medulla and lobula lie distal to the voluminous reniform body. Whereas mushroom body neuropils, here represented by one column, contain systems of anti-TH-positive neurons, as do medulla and lobula neurons associated with the stomatopod's retinal midband (Figure 2a), the reniform body appears to entirely lack anti-TH-immunoreactive elements. This is an important distinction when comparing observations of other species (see Section 5).

Immunostaining with anti-α-tubulin (Figure 2b) shows extensive projections by tracts into the reniform body neuropil, each tract providing numerous tributaries extending into four discrete domains. These are delineated by, among other features, their specific affinities to 5HT antibodies (Figure 2c) and to antibodies raised against GAD (Figure 2d). These domains further correspond to the terminal branches of single Golgi-impregnated neurons (Figure 2e). The affinity of the reniform body to antibodies raised against DC0 (Figure 2f–h) varies across specimens in contrast to the uniformly intense anti-DC0 affinity of the mushroom body's columns. In the moderately labeled reniform bodies, co-labeled with anti-α-tubulin, DC0 antibodies demonstrate successive gyri, each corresponding to a domain revealed by anti-GAD or anti-5HT in Figure 2c, d. These distinctions are further emphasized by their delineation of sulcus-like fissures (Figure 2f). In some specimens, the pattern of immunoreactivity suggests that the DC0 epitope can be specifically localized within fiber tracts extending into these domains (Figure 2g, h), an impression strengthened by immunoreactivity also localized to the reniform body's pedestal (Figure 2g), which comprises axons extending from rostral cell bodies to its ventral neuropils (Wolff et al., 2017).

Of special note are the large ovoid territories delineated by anti-GAD immunohistology (Figure 2d). These correspond to systems of synaptic baskets (see Section 3), the formations of which are so prominent as to be visible as outswellings from the reniform body surface (Figure 3a, b). Immunostaining with the synaptic marker SYNORF1 and low power confocal scanning of the whole lateral protocerebrum reveals these features as prominently as it does the medulla's midband protuberance, representing the compound eyes' retinal midband (Thoen et al., 2018). The dense covering of the calyces by the mushroom body's globuli cells is also shown in Figure 3a. The synaptic baskets are not only the most prominent substructures of the reniform body but are the first to demonstrate its connection to a lateral domain of the lobula. Fills using dextran-Texas red injected into the lobula demonstrate that together these aggregated baskets comprise a considerable volume of neuropil, as resolved by the color-coded depth map in Figure 3c.

As remarked above, comparisons of Bodian-stained brains identify corresponding organization of reniform bodies across Stomatopoda, here exemplified by two specimens of *G. smithii* and *G. chiragra* (Figure 3d, e). Double-impregnation by the Golgi method results in en masse staining of neurons, providing further insight into the dendritic morphologies of the reniform body's initial zone (Figure 3f, g). This zone is connected by a columnar-like pedestal composed of parallel axons extending to the reniform body's caudal expansion into its four adjoining domains, each of which can be resolved by its affinity to anti-DC0 (Figure 3h).

4.2 | Connections of the optic lobes to the reniform and mushroom bodies

Although there are still challenges to using fluorescent tracers on marine arthropods—one being the fragility of the tissue and another the difficulty of keeping the animal oxygenated during the filling period—application of dyes to the stomatopod's lobula and

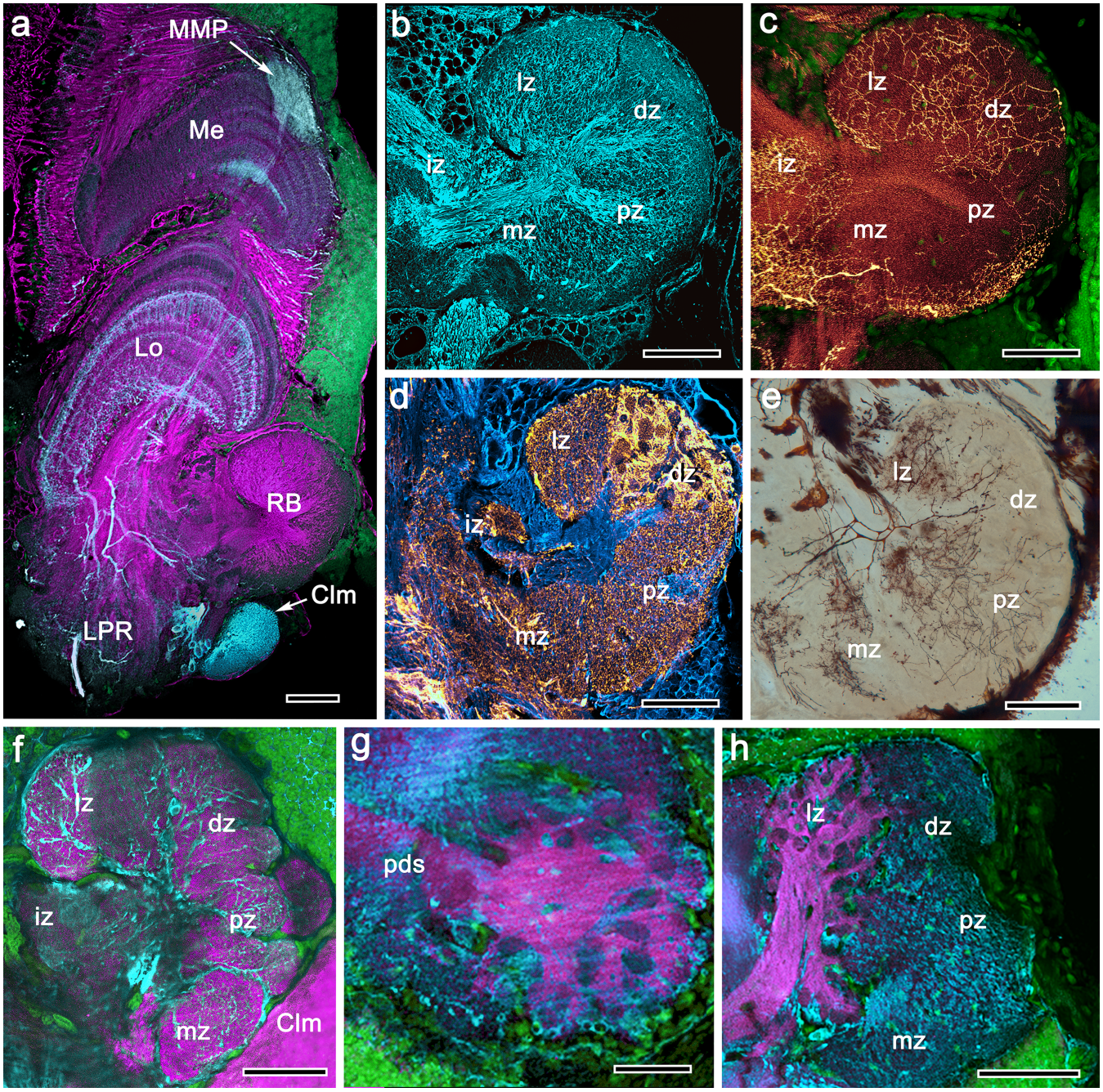

FIGURE 2 Location and architecture of the reniform body in *Neogonodactylus oerstedii*. (a) The right lateral protocerebrum (LPR) immunostained using anti-α-tubulin (magenta), anti-TH (cyan) with neuronal cell bodies stained using Syto13. Anti-TH resolves systems of through-going and tangential processes associated with the optic lobe's representation of the retinal midband, such as the medulla midband protuberance (MMP; see, Thoen, et al., 2018). Anti-TH also resolves part of one of the mushroom body columnar lobes (Clm). Notably, the reniform body (RB) shows no affinity for anti-TH, in contrast to the anti-TH-receptive components of the mushroom body. (b) Reniform body labeled with anti-α-tubulin showing major tracts fanning out from the initial zone (iz) into four discrete domains: the lateral, distal, proximal, and medial zones (lz, mz, pz, and mz). (c) anti-5HT (orange) and (d) anti-GAD (yellow) immunoreactivity demonstrate that each zone has a characteristic immunoreactive signature (blue: α-tubulin). Of special note are the dense arborizations of 5HT-immunoreactive processes in the lz and dz (c), and the perforated aspect of crowded anti-GAD immunoreactivity (d) in the distal zone (dz). (e) Certain axon terminals entering the caudal neuropils of the reniform body send branches into all its zones (contrast with Figure 3g). (f–h) Various distributions in the reniform body's caudal neuropil of anti-DC0 (magenta) immunoreactivity (cyan: α-tubulin). In (f) all zones are DC0-immunoreactive, distinguished by their swollen perimeters and sulci-like indentations; whereas in (g) the pedestal (pds) and its diverging tributaries or, in (h), a major tract from the lateral protocerebrum, express DC0 immunoreactivity. Lo, lobula; Me, medulla. Scale bars: a, 200 μm; b–h, 100 μm

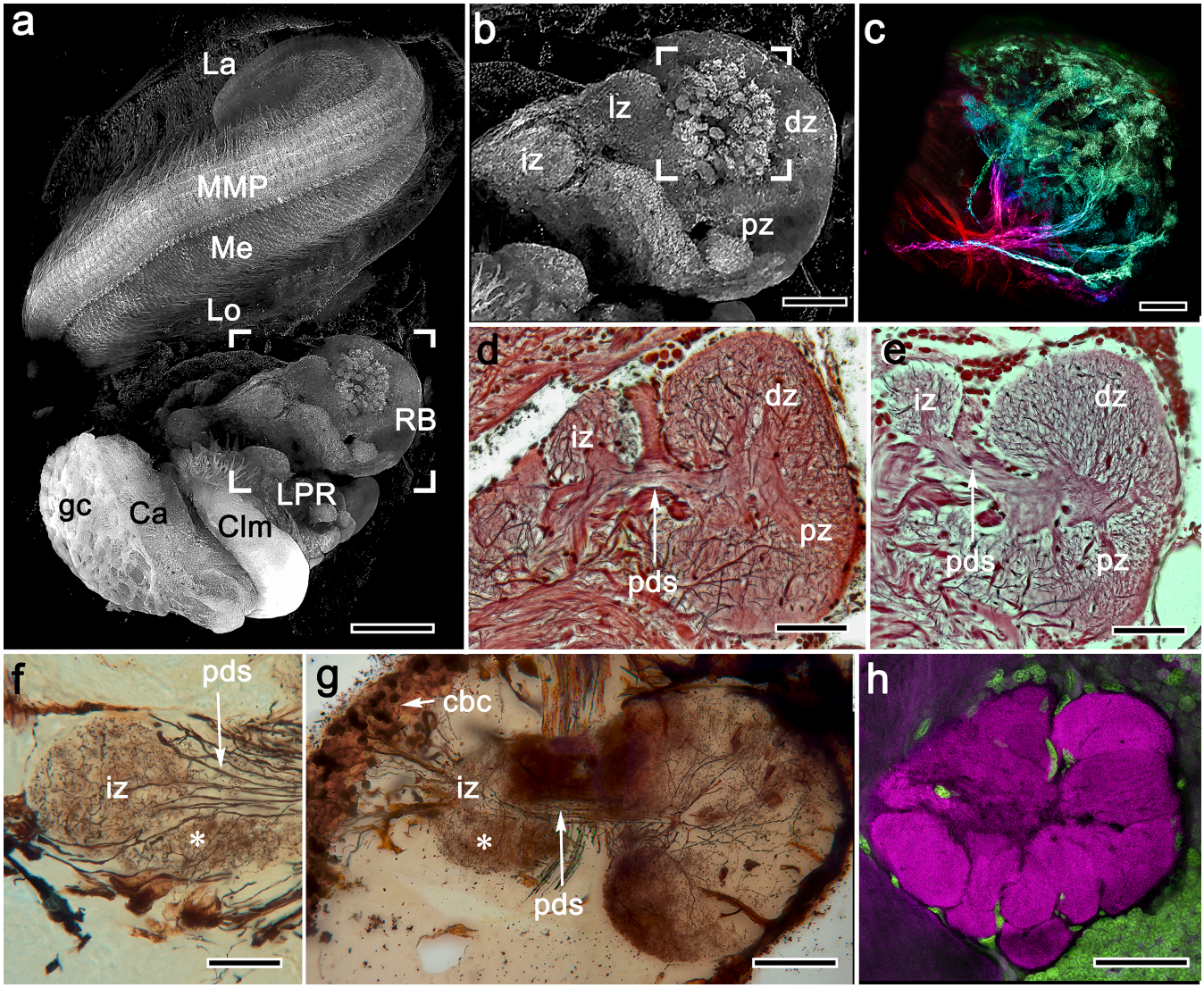

FIGURE 3 The stomatopod reniform body. (a) Low-power confocal scan of an intact optic lobe and lateral protocerebrum immunolabeled with anti-SYNORF. The raised profile of the medulla midband protuberance (MMP) representing the retina's chromatic midband is clearly distinguished from flanking areas of the medulla (Me) that almost completely overhang the lobula (Lo) beneath. The reniform body (bracketed RB) and deeper neuropils of the lateral protocerebrum (LPR) are prominent features, as is a region of mid-size glomeruli in the reniform body. The mushroom body calyx (Ca) is shown capped by its population of globuli cells (gc) and, beneath it, one of its two largest columnar lobes (Clm). (b) Enlargement of boxed area in panel (a) showing surface features of the reniform body zones. The bracketed area indicates the glomerular subunits that characterize this zone, and that correspond to the perforations of anti-GAD-immunoreactive processes shown in Figure 2d. (c) A confocal depth-coded scan of Texas red fills of the glomerular subunits after application of the dye to the inner lobula. (d,e) Comparison of reniform bodies in two stomatopod species, *Gonodactylus smithii* and *Gonodactylus chiragra*. (f) Detail of the initial zone (iz) of the reniform body showing its small satellite arborization (asterisk). (g) Overview of a Golgi-impregnated reniform body in *N. oerstedii*, showing the cell body cluster (cbc) supplying neurons that link the initial zone (iz) with its caudal volume. (h) Intensely anti-DC0-labeled caudal zones of the reniform body used for comparison with perimeters defined by other markers, as shown in Figure 5b. La, lamina; pds, pedestal. Scale bars: a, 200 μm; b, 100 μm; c, 20 μm; d, e, 100 μm; f, 50 μm; g, h, 100 μm

reniform body has provided three important findings (Figures 4a and 8). The first is that connections diverge from the lobula both directly and indirectly to at least six target areas in the lateral protocerebrum, all of which belong to higher order integration centers. The most prominent of these connections is one providing the cluster of synaptic baskets in the reniform body's distal zone, which are provided by more than a dozen bundled axons (Figure 4a, b). The second finding is that the same dye application site also reveals pathways that extend to the mushroom bodies. Two of these penetrate the largest mushroom body column at two locations beneath the calyces (Figure 4c). Third, two additional terminal fields extend across the inner calycal layer (Figure 4d, g) and at a level immediately above it at the origin of its columnar lobe (Figure 4e, f, h). These terminals do not, however, originate in the lobula but are revealed by Texas red

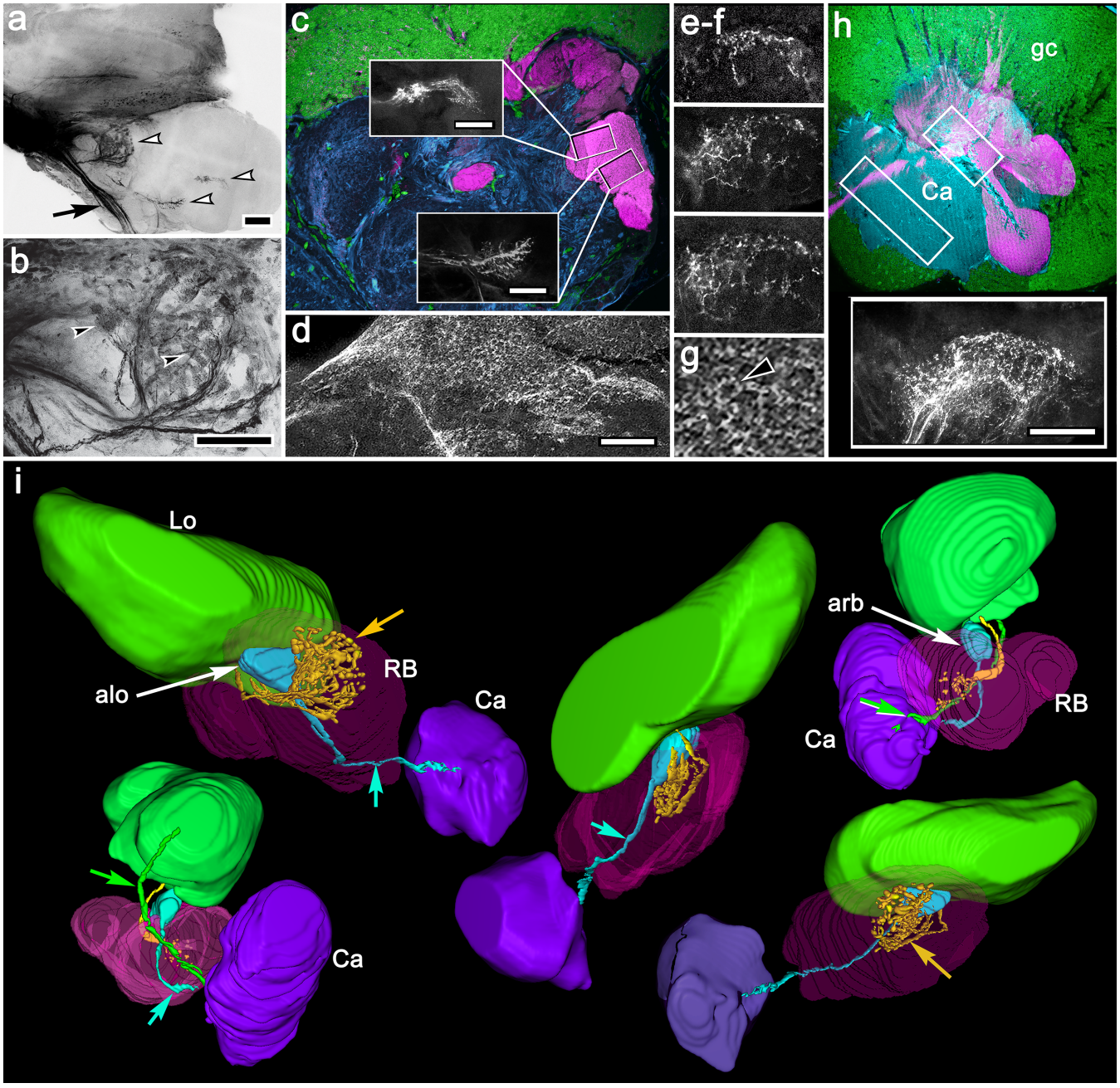

FIGURE 4 Texas red fills into the stomatopod lobula (Lo) and reniform body (RB). (a) Results of a fill into the base of the lobula showing a tract from it extending centrally into the lateral protocerebrum (arrowed) and three other tributaries diverging to the glomerular distal zone (upper arrowhead) and to two levels in the mushroom body lobes (middle and lower arrowheads). (b) Enlargement of glomerular subunits (e.g., at black arrowheads) marked by upper arrowhead in (a). (c) Anti-DC0-labeled (magenta) lobe of the mushroom body. Insets show Texas red-filled terminals and their location along the columnar lobe. (d) Terminals in the mushroom body calyx from a tract filled by Texas red injection into the reniform body. The terminals occupy a broad swathe of the calyx, in which crown-like terminal specializations correspond to calycal microglomeruli described in Wolff et al., (2017), one indicated by the arrowhead in panel g. (e–f) Serial confocal optical sections through a system of terminals, filled by Texas red injected into the reniform body, that extend across the roots of the mushroom body lobes. (h) The location of a reconstructed terminal (monochrome inset) is indicated by the box over the mushroom body calyx (cyan: anti-α-tubulin) and the origin of its lobes (magenta: anti-DC0). The elongated box across the calyx (Ca) indicates an area corresponding to a scan of the terminals shown in panel d. (i) Views of a three-dimensional reconstruction of Texas red fills into restricted volumes of the inner lobula or reniform body (cyan) (for video depiction see Supplementary Information). Glomerular units (yellow arrows); tracts to mushroom body lobe (green arrows), tracts to mushroom body calyx (cyan arrows); dye injection sites at the lobula (alo) and reniform body (arb). Other abbreviations: gc, globuli cell; Lo, lobula. Scale bars: a, b, 50 μm; c insets, 50 μm; d, 50 μm; h inset, 50 μm

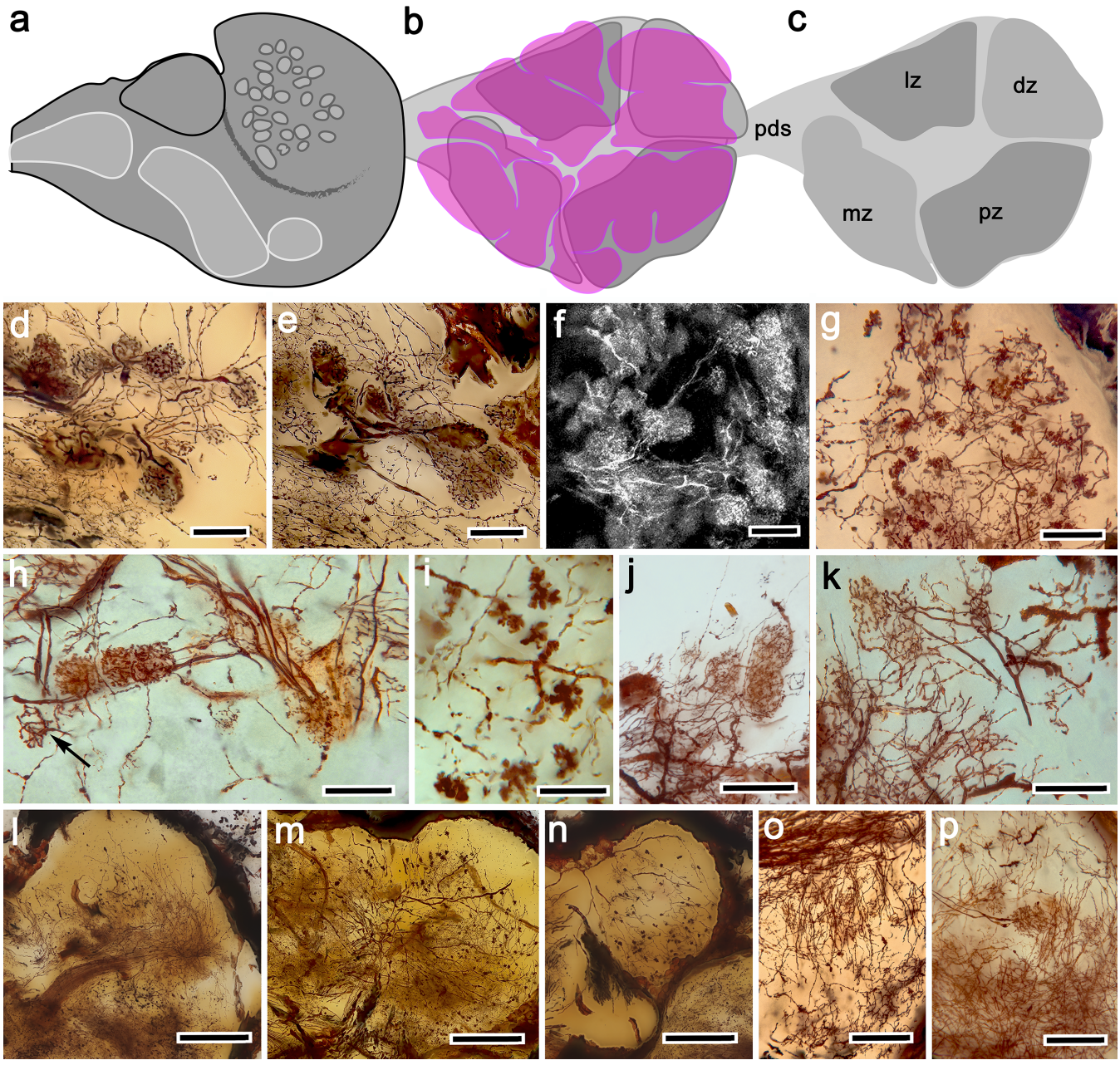

FIGURE 5 Neuronal configurations in the stomatopod reniform body showing relationships with zones. (a) Intact reniform body visualized by anti-synapsin. (b) Anti-DC0-immunoreactive domains aligned with innervation patterns in panel c, which indicates the pedestal (pds), lateral, distal, proximal, and medial zones. (d, e) Golgi-impregnated basket and pocket specializations correspond to units filled by Texas red applied to the lobula shown in panel f. (g) Morphologies characterizing specializations from the same initial arbor allow distinctions of different terminal types. (h) Linearly arranged dendritic baskets with a coarser varicose formation suggesting a corresponding presynaptic element (arrow). (i) Detail of dense varicose specializations, originating from a terminal arbor in the lateral zone, matching the dimensions of smaller pockets shown in panels j and k. (l, m) Massive bundles of extremely thin axons extending into the reniform body suggest the participation of hundreds of neurons originating from lateral protocerebral neuropils. (n) A diffuse arrangement of small beaded terminals from a slender afferent fiber extending into the lateral zone. (o) A population of incoming afferents to the medial zone provides ranked branches ascending toward the mz surface. (p) Tangles of incoming processes intermingle with clearly defined microglomerular arrangements. Scale bars: d–f, 25 μm; g, 50 μm, h–k, 25 μm; l–n, 100 μm; o, p, 25 μm

application into the reniform body, at a location that also resolves microglomeruli in its distal zone. Serial reconstructions of these centers and three-dimensional views of these projections (Figure 4i and Video S1) further demonstrate that the stomatopod mushroom body can no longer be considered as simply a higher olfactory center. It also integrates information from the lobula directly and indirectly via neurons originating in the reniform body. This is further considered in the Discussion.

4.3 | Further details of reniform architecture

Three different observational strategies demonstrate that the reniform body is highly elaborated: (a) matching anti-DC0-immunoreactive domains with innervation patterns (Figure 2b–d); (b) imaging of the intact reniform body visualized by anti-SYNORF1 (Figure 3a); and (c) relating aminergic organization to discrete zones (Figure 5a–c). The latter organization is not as clear cut as might be suggested because as shown in Figure 2e, single axons to or from the reniform body can send branches into all its zones. Conversely, arborizations from other tracts are clearly seen to be limited to within a zone, as indicated by mass Golgi impregnation shown in Figure 3g. Golgi impregnations show that in the distal zone, dendritic and terminal specializations vary in size, suggesting two sizes of intermingling synaptic baskets and pockets (Figure 5d–f). Their clasp-like processes are not obviously distinguishable as functionally dendritic or terminal, however. Endings from the dye-filled lobula tract appear to have varicose branches that are distinct from synaptic pockets of similar size, but equipped with dense claw-like clusters (Figure 5f). And, whereas in the distal zone synaptic baskets are spaced quite far apart, in the lateral zone the smaller synaptic pockets are more crowded and their putative pre- and post-synaptic elements can be readily distinguished (Figure 5h). Certain arborizations providing terminal processes show characteristic morphologies and distributions originating from the same initial arbor (Figure 5g). Dense varicose aggregations, as in Figure 5i, match the dimensions of the smaller and most delicate pockets, like those depicted in Figure 5j, k.

Specimens in which whole axon bundles have been impregnated into the reniform body suggest the participation of hundreds of neurons, as inferred from the bundles shown in Figure 5l, m. Not all afferents terminate as swellings, however, and not all putative outputs have dendritic trees equipped with synaptic baskets or pockets. Dozens of incoming afferents to the medial zone, for example, give rise to ranked branches that ascend toward the surface of the neuropil (Figure 5o). Others, as in the proximal and distal zones, provide tangles of processes that intermingle with clearly defined arrangements of synaptic pockets.

4.4 | The varunid reniform body: The description

An earlier study (Wolff et al., 2017) demonstrated that the reniform body is not unique to Stomatopoda but also exists in Brachyura, one of the youngest branches of decapod crustaceans. The striking similarity of these centers in these taxa is demonstrated by comparing Figures 3g and 6c. These Golgi impregnations reveal structural correspondences pertaining to a rostral cell body cluster that supplies a columnar pedestal, from which arise four discrete territories composed of densely branched collaterals. As for the stomatopod, in the crab these are termed the initial zone (iz) and four adjoining caudal domains: the lateral, distal, proximal, and medial zones (lz, dz, pz, and mz). Also, as in the stomatopod, the reniform body of the shore crab (Figure 6a–f) originates from a cluster of very small perikarya lying over the rostro-dorsal surface of the lateral protocerebrum, just proximal to the inner border of the lobula (Figure 6a, b). Many of these cell bodies are intensely labeled by anti-DC0 antibodies as are the neuronal processes they supply and that supply arborizations to the aforementioned zones (Figure 6a). The zones revealed by anti-DC0 labelling (Figure 6a) match exactly the organization revealed by Golgi impregnations of their constituent neurons (Figure 6c).

The trajectory of the reniform body's pedestal extends obliquely from its rostro-dorsal origin toward the more ventrally disposed caudal zones. This means that the entire reniform body cannot be resolved within a single vertical plane of section but only in a section cut parallel to its pedestal's long axis, as shown in Figure 6a, b. When the rostral portion of the pedestal is resolved, as in Figure 6d where it is accompanied by the entire extent of the initial zone, the more caudal parts of the reniform body are out of the section and thus not visible.

Some ambiguity relates to extensive anti-DC0-positive neuropils resolved proximal to the reniform body. Despite their morphological distinction from anti-DC0 immunoreactive centers in achelate brains, these neuropils have been designated as "hemiellipsoid bodies" (Krieger et al., 2015). Here, we continue to use this terminology despite it being problematic. Cell bodies supplying intrinsic neurons of these extensive centers, like those supplying the reniform body, are clustered over the rostral and rostro-dorsal surfaces of the lateral protocerebrum. However, these centers cannot be assumed to have evolutionarily derived from an organization that typifies anti-DC0 immunoreactive centers in achelate and astacid lineages (Blaustein, Derby, Simmons, & Beall, 1988). In the varunid crab, such anti-DC0 territory may (but not invariably) occupy substantial volumes of the lateral protocerebrum, as indicated by asterisks in Figure 6b, d–f, the maximum observed denoted in Figure 6e. The largest volumes are reminiscent of the massive, and folded, mushroom body lobes identified in whip scorpions belonging to the arachnid Amblypygi (Wolff & Strausfeld, 2015). A facile suggestion for the observed size differences is that they reflect different levels of DC0 upregulation, the strength of which reflects the volume of sensory associations being processed by them at the time of cold anesthesia and fixation.

4.5 | The varunid reniform body: A correction

Corresponding neuronal arrangements in the stomatopod and varunid reniform bodies described in Wolff et al. (2017), referred to panels a–d in Figure 6 of that publication. These demonstrate the dispositions of perikarya, such as the reniform body's cell body cluster (cbc), the prolongations of which provide fibers of the pedestal. This arrangement is shown as identical in the stomatopod and varunid reniform bodies. While the explanation of those depictions is correct, two additional panels (loc. cit. H and I) are misleading. They show two clusters of cell bodies disposed on opposite surfaces of the lateral protocerebrum, both of which include DC0-positive perikarya. One cluster (annotated in the 2017 paper as hbc) lies over the rostral surface and was correctly ascribed to the crab's hemiellipsoid body neuropils. The other cluster (cbc) is shown to lie above the caudal side of

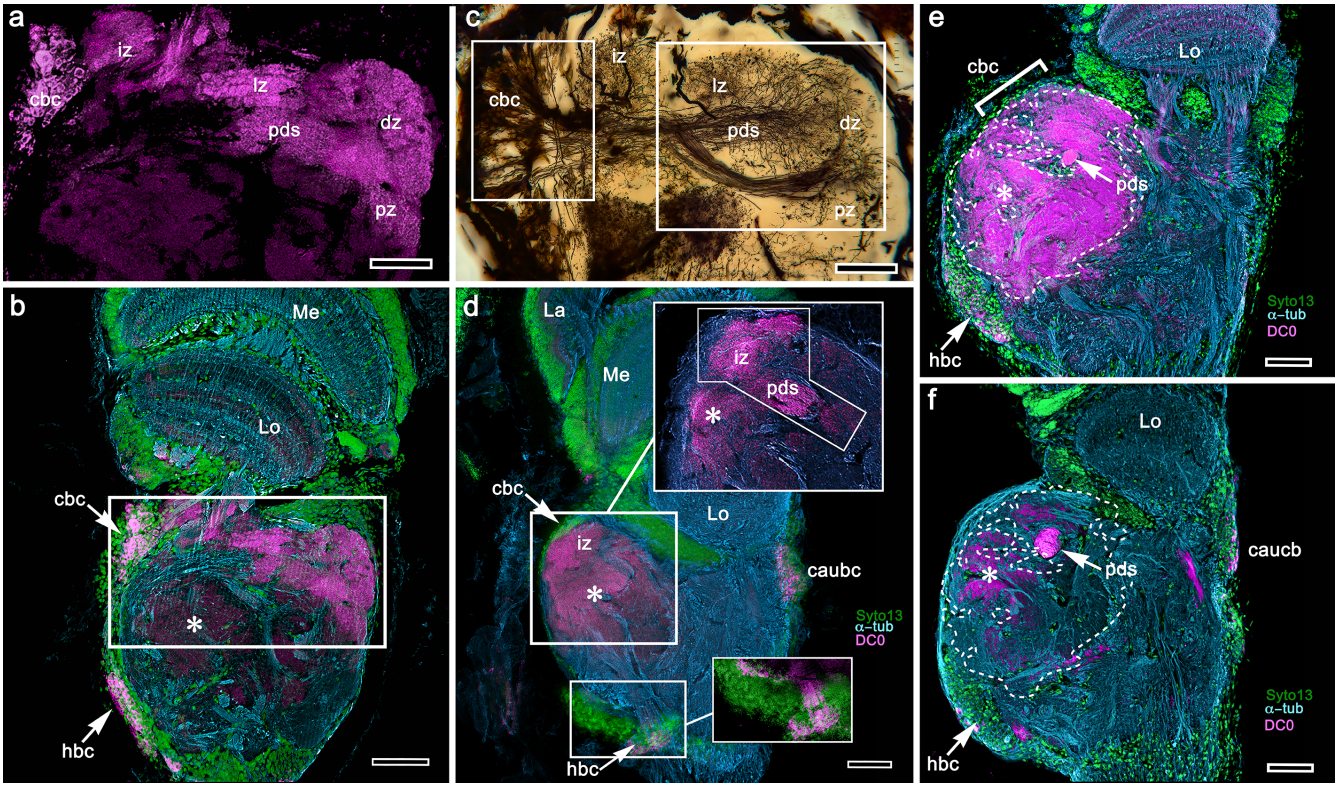

FIGURE 6 Reniform body of the shore crab, *Hemigrapsus nudus*. In these lengthwise sections of the lateral protocerebrum rostral is to the left in each panel, distal is upward. (a) Distribution of anti-DC0-positive cell bodies (cbc), pedestal (pds) and processes that are constrained to the initial, lateral, distal, and proximal zones (iz, lz, dz, and pz). (b) Overview of the section that includes most of the reniform body's extent. The boxed area corresponds to panel a. Anti-DC0-positive cell bodies are resolved in cbc and among cell bodies (hbc) supplying hemiellipsoid body neuropils (asterisk). (c) Golgi-impregnated reniform body showing dendritic and terminal zones that closely correspond to those demonstrated for the stomatopod (see Figure 3h) that exactly match anti-DC0 profiles in panel a. A cluster of rostral cell bodies (cbc) provides axons of the pedestal (pds) from which arise the dense arborizations of the initial, lateral, distal, and proximal zones (iz, lz, dz, and pz). (d) A specimen of *H. nudus* showing cell bodies in a corresponding rostral cell body cluster (cbc), part of a distributed population of cell bodies many of which (hbc, boxed and enlarged) are associated with hemiellipsoid body anti-DC0-positive domains. The middle boxed area in panel d is enlarged to demonstrate anti-DC0-positive neuropils belonging to the reniform body initial zone and pedestal (outlined by irregular polygon). A distinctive caudal cluster of neuronal cell bodies (caubc) also reveals anti-DC0-positive perikarya. (e, f) Two sections of the lateral protocerebrum showing the intensely anti-DC0 labeled pedestal (pds in c, d). These two panels also demonstrate maximum and minimum levels of anti-DC0 immunoreactivity of the varunid hemiellipsoid body. Its maximum extent, outlined in e, is shown superimposed on the lateral protocerebrum in panel f where anti-DC0 labelling is minimal and patchy. Asterisks in panels b and c similarly indicate various levels of anti-DC0-immunoreactivity of hemiellipsoid body neuropils. All scale bars = 50 μm

the lateral protocerebrum. This latter identification is incorrect as it erroneously places the cbc at the caudal surface of the lateral protocerebrum, whereas Golgi and Bodian reduced-silver stains now clearly show the reniform body as deriving from cell bodies lying over its rostral surface (Figure 6). The cell bodies providing the reniform body retain their identity as the cbc. The cluster of cell bodies over the caudal surface of the lateral protocerebrum, which also includes perikarya immunoreactive to anti-DC0, is now designated as the caudal cell body cluster (caucb).

5 | DISCUSSION

5.1 | Reniform bodies are not mushroom bodies

In *H. nudus*, the olfactory glomerular tract distributes its terminal branches to a variety of neuropils in the lateral protocerebrum. Many of these show medium-to-intense affinity to anti-DC0 labelling (see Figure 6a, b, d–f), suggesting these territories belong to a large "hemiellipsoid body" as well as some anti-DC0-positive satellite neuropils associated with it, as in Astacidea and Achelata (Strausfeld & Sayre, 2019). In *H. nudus*, small cell bodies lying over the rostral surface of the lateral protocerebrum are associated with those volumes and a subset of them close to the lobula supplies the intrinsic neurons of the reniform body. This corresponds to organization in Stomatopoda: the cluster of rostrally disposed cell bodies near the inner margin of the lobula that supplies the reniform body is adjacent to the much larger cluster of some thousands of cell bodies that supplies the mushroom body intrinsic neurons. Thus, as shown in Figure 7, all the topography of the mushroom body and reniform body in Stomatopoda correspond to those in shore crabs. This similarity strongly suggests that the center described by Maza et al. (2016) as a "mushroom body" in the crab *N. granulata* is neither a mushroom body

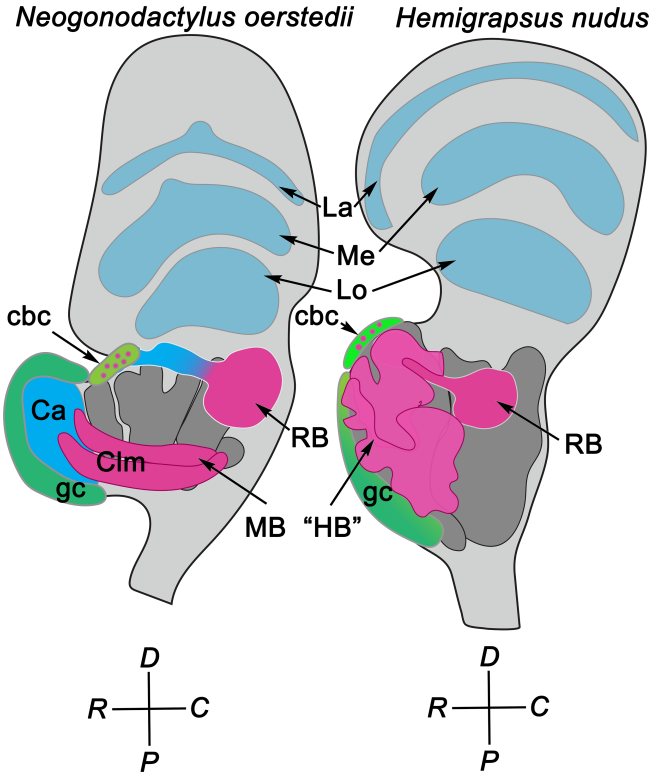

FIGURE 7 Schematic comparison of the stomatopod *Neogonodactylus oerstedii* and the varunid shore crab *Hemigrapsus nudus* to show their corresponding dispositions of reniform body (RB) in relation to the mushroom body (MB) and its evolved derivative, the hemiellipsoid body (HB). Other abbreviations: La, lamina; Me, medulla; Lo, lobula; gc, globuli cell layer; D, distal, P, proximal, R, rostral, C, caudal

nor its evolved modification, the hemiellipsoid body. In the crab, the center referred to as the hemiellipsoid body is represented by a distinct neuropil complex denoted by extensive volumes immunoreactive to anti-DC0 (Figure 6a, b, d–f).

A number of other features distinguish the reniform body from the mushroom body. One is that the reniform body's pedestal and caudal neuropils appear to be free of immunoreactivity to antibodies raised against TH, whereas in *N. oerstedii* anti-TH-immunoreactive zones characterizing the mushroom body's columnar lobes (Wolff et al., 2017) indicate dendritic territories of mushroom body output neurons, as they do in *Drosophila* and the cockroach (Cohn, Morantte, & Ruta, 2015; Hamanaka, Minoura, Nishino, Miura, & Mizunami, 2016). A second distinguishing feature is that the reniform body's pedestal comprises smooth axons that show none of the synaptic specializations that typify the extended processes of intrinsic neurons comprising the length of a mushroom body's columnar lobe, as observed in Stomatopoda, Caridea, Paguroidea, and insects (Sayre & Strausfeld, 2019; Strausfeld, Sinakevitch, Brown, & Farris, 2009; Wolff et al., 2017). Third, the prominent arrangement of caudally placed adjoining zones that extend from the pedestal share none of the morphological attributes of columnar lobes typifying mushroom bodies. Finally, the reniform body's initial zone has no resemblance to a calyx. These observations are disparate to Maza et al. (2016) and interestingly these authors show compelling evidence that the *N. granulata* reniform body participates in context-dependent visual memory. This observation, we would suggest, further aligns this center in the crab with our present observations of the stomatopod reniform body, demonstrating its unambiguous connections to the visual system's lobula and to the mushroom bodies.

5.2 | Functional relevance

One result of this study has been the distinction of the reniform body with respect to its connections with the visual system's lobula and with the mushroom body. Thus far, evidence suggests that various tracts in the lateral protocerebrum provide the reniform body with its connections. But, we do not yet know which modalities these centers serve. That the reniform body is so richly supplied with inputs, and its intrinsic composition is so elaborate, suggests that this center integrates multisensory information that is already highly processed before it reaches the reniform body circuits. The exception, as suggested by dye fills, is the reniform body's direct input from the lobula.

Dye fills into the reniform body and from it to the mushroom bodies are summarized in Figure 8. The reniform body's connections to the mushroom body include terminals supplying the inner layer of the calyces and a set of endings penetrating the interface between calycal neuropil and the roots of the emerging mushroom body columns. These are levels where intrinsic neurons begin their elongations through serially arranged orthogonal circuits spaced sequentially along the columns (Wolff et al., 2017).

These connections to the mushroom body suggest similarities with an organization in the insect lateral protocerebrum, where the mushroom bodies and their calyces do not simply receive sensory relays from the optic lobes and the olfactory lobes but are also supplied by connections from the lateral protocerebrum. As first shown in locust and cockroach brains, mushroom body calyces receive a variety of inputs, usually inhibitory, originating from a rostral assemblage of neuropils collectively called the lateral horn, which is situated between the mushroom body and the lobula (Schildberger, 1984; Strausfeld, 1976, 2012; Strausfeld & Li, 1999; Yamazaki, Nishikawa, & Mizunami, 1998). Neurons from the lateral horn have been demonstrated to play pivotal roles in the segregation and parceling out, or sparsening, of information represented by small groups of Kenyon cells, the axon-like fibers that extend into the mushroom body columns (Perez-Orive, Mazor, Turner, Cassenaer, Wilson, & Laurent, 2002), and in interacting with mushroom body outputs in the assessment of valence (Dolan, Frechter, Bates, Dan, Houviala, Roberts, et al. 2019). We suggest that, if the evolution of the reniform body has persisted through to the allotriocarid branch of Pancrustacea, then regions such as the lateral horn, which also receives inputs from optic glomeruli and the lobula, in addition to those from the antennal lobes (Galizia & Rössler, 2010; Strausfeld, Sinakevitch, & Okamura, 2007), may provide useful search images for investigating possible roles of the stomatopod reniform body.

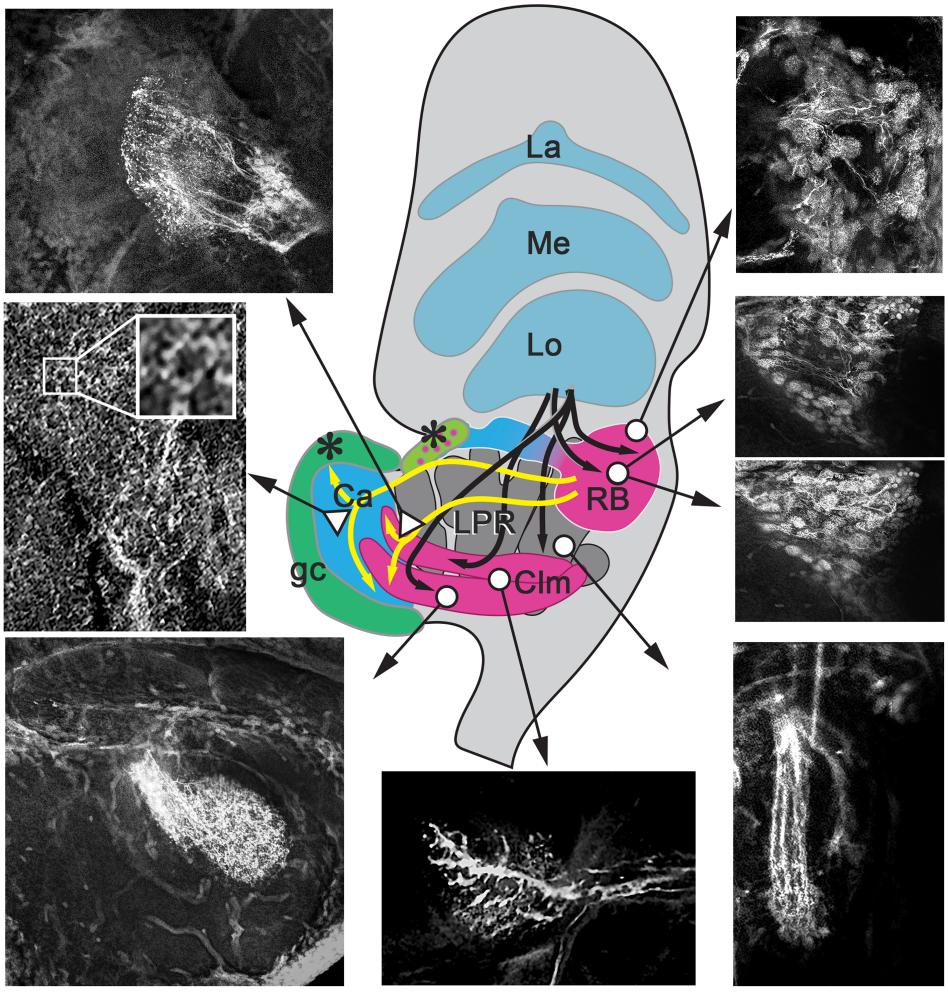

FIGURE 8 Summary figure showing the presently known connections between the lobula (Lo), the reniform body (RB), and the mushroom body (Ca + Clm). Black lines indicate fills from dextran-conjugated Texas red applied to the lobula and yellow lines indicate fills from the reniform body. Arrows from white circles indicate the relevant confocal images of terminals filled with dextran-conjugated Texas red applied to the lobula. Arrows from white triangles indicate terminals and their locations after applying the tracer to the reniform body. Fills from the lobula demonstrate a direct connection to the reniform body, supplying distinct clusters of synaptic pockets and synaptic baskets in the distal and lateral zone (top three pictures on right). The lobula also has connections terminating in a discrete neuropil, possibly equivalent to an insect optic glomerulus, in the lateral protocerebrum (LPR; bottom right), as well as providing the mushroom body columns (Clm) with input (bottom middle and left). Dye fills into the reniform body show its direct connections with the mushroom body through pathways both to its columns and its inner calycal (Ca) layer (top two pictures on left). Inset in middle left shows the enlargement of crown-like terminal specializations similar to those described in Wolff et al. (2017). Asterisks indicate the cell bodies of the reniform body (light green) and the mushroom body (darker green), respectively. Medulla (Me) and lamina (La) shown above the lobula for illustration

Another important finding here, which further aligns the stomatopod mushroom body with that of insects, is that its lobes receive inputs from the lobula. As described from insects, inputs from the lobula and medulla supply the calyces, and neurons terminating in the columnar lobes also encode visual information (Ehmer & Gronenberg, 2002; Lin & Strausfeld, 2012; Paulk & Gronenberg, 2008; Vogt et al., 2016). Thus, the stomatopod mushroom body's relationship with other higher centers and with sensory systems other than those encoding chemosensory information are not exceptional but may typify mushroom bodies in general.

To summarize, we have shown that the stomatopods have a prominent neuropil in their lateral protocerebrum, the reniform body, which is connected to both the lobula and the mushroom body, suggesting it is involved in the integration of multisensory information. Similar centers have been identified in varunid crabs described here, in the caridean *L. groenlandicus*, and the marine hermit crab *P. hirsutiusculus* (Sayre & Strausfeld, 2019; Strausfeld & Sayre, 2019), showing that across Eumalacostraca some, if not all, decapod lineages possess two higher centers (the reniform body and the mushroom body) likely to be involved in learning and memory. The implications of this and the functional relevance of the reniform body have yet to be discovered, but could possibly be revealed by studying the behavioral differences as well as the ecological constraints of these species.

ACKNOWLEDGMENTS

The research described here is supported by the National Science Foundation under Grant No. 1754798 awarded to N.J.S., as well as the University of Arizona's Center for Insect Science, and funding from the University of Arizona Regents Fund. Support for H.H.T. and J.M. came from grants awarded by the Asian Office of Aerospace Research and Development (AOARD-12-4063) and the Australian Research Council (FL140100197), and a Doctoral Fellowship (2013) to H.H.T. from the Lizard Island Research Foundation and the Lizard Island Research Station, a facility of the Australian Museum. Our gratitude goes to Daniel Kalderon, Columbia University, New York, for supplying the DC0 antibody. We have profited from discussions with Charles Derby (Georgia State University, Atlanta), who read and commented on the manuscript. And, we are indebted to Camilla Strausfeld for critically discussing and meticulously editing the text.

DATA AVAILABILITY STATEMENT

Confocal images pertaining to this research are maintained on the investigators' storage devices. Immunostained specimens and Golgi-impregnated specimens are maintained in the Marshall Laboratory, University of Queensland and in the Strausfeld Laboratory, University of Arizona.

ORCID

Hanne Halkinrud Thoen https://orcid.org/0000-0001-8695-9578
Gabriella Hannah Wolff https://orcid.org/0000-0002-0075-4975
Justin Marshall https://orcid.org/0000-0001-9006-6713
Marcel E. Sayre https://orcid.org/0000-0002-2667-4228
Nicholas James Strausfeld https://orcid.org/0000-0002-1115-1774

REFERENCES

Andrew, D. R., Brown, S. M., & Strausfeld, N. J. (2012). The minute brain of the copepod *Tigriopus californicus* supports a complex ancestral ground pattern of the tetraconate cerebral nervous systems. *Journal of Comparative Neurology*, *520*, 3446–3470. https://doi.org/10.1002/cne.2309

Antonsen, B. L., & Paul, D. H. (2001). Serotonergic and octopaminergic systems in the squat lobster *Munida quadrispina* (Anomura, Galatheidae). *Journal of Comparative Neurology*, *439*, 450–468. https://doi.org/10.1002/cne.1362

Bellonci, G. (1882). Nuove ricerche sulla struttura del ganglio ottico della *Squilla mantis*. *Memorie della Accademia delle Scienze dell'Istituto di Bologna, Serie 4*, *3*, 419–426.

Blaustein, D. N., Derby, C. D., Simmons, R. B., & Beall, A. C. (1988). Structure of the brain and medulla terminalis of the spiny lobster *Panulirus argus* and the crayfish *Procambarus clarkii*, with an emphasis on olfactory centers. *Journal of Crustacean Biology*, *8*, 493–519. https://doi.org/10.2307/1548686

Bodian, D. (1936). A new method for staining nerve fibers and nerve endings in mounted paraffin sections. *Anatomical Record*, *69*, 153–162. https://doi.org/10.1002/ar.1090650110

Brauchle, M., Kiontke, K., MacMenamin, P., Fitch, D. H. A., & Piano, F. (2009). Evolution of early embryogenesis in rhabditid nematodes. *Developmental Biology*, *335*, 253–262. https://doi.org/10.1016/j.ydbio.2009.07.033

Chiou, T.-H., Kleinlogel, S., Cronin, T. W., Caldwell, R., Loeffler, B., Siddiqi, A., & Marshall, N. J. (2008). Circular polarization vision in a stomatopod crustacean. *Current Biology*, *18*, 429–434. https://doi.org/10.1016/j.cub.2008.02.066

Cohn, R., Morantte, J., & Ruta, V. (2015). Coordinated and compartmentalized neuromodulation shapes sensory processing in *Drosophila*. *Cell*, *163*, 1742–1755. https://doi.org/10.1016/j.cell.2015.11.019

Cournil, I., Helluy, S. M., & Beltz, B. S. (1994). Dopamine in the lobster *Homarus gammarus*. I. Comparative analysis of dopamine and tyrosine hydroxylase immunoreactivities in the nervous system of the juvenile. *Journal of Comparative Neurology*, *334*, 455–469. https://doi.org/10.1002/cne.903440308

Crisp, K. M., Klukas, K. A., Gilchrist, L. S., Nartey, A. J., & Mesce, K. A. (2001). Distribution and development of dopamine- and octopamine-synthesizing neurons in the medicinal leech. *Journal of Comparative Neurology*, *442*, 115–129. https://doi.org/10.1002/cne.10077

Cronin, T. W., & Marshall, N. J. (1989). A retina with at least ten spectral types of photoreceptors in a mantis shrimp. *Nature*, *339*, 137–140. https://doi.org/10.1038/339137a0

Dolan, M.-J., Frechter, A., Bates, A. S., Dan, C., Huoviala, P., Roberts, R. J. V., … Jefferis, G. S. X. E. (2019). Neurogenetic dissection of the *Drosophila* lateral horn reveals major outputs, diverse behavioural functions, and interactions with the mushroom body. *eLife*, *2019*(8), e43079. https://doi.org/10.7554/eLife.43079

Ehmer, B., & Gronenberg, W. (2002). Segregation of visual input to the mushroom bodies in the honeybee (*Apis mellifera*). *Journal of Comparative Neurology*, *451*, 362–373. https://doi.org/10.1002/cne.10355

Facchini, C. (1890). *Biografia di Guiseppe Bellonci e Indice de'suoi lavori*. Bologna: Società Tipografica Azzoguidi.

Galizia, G., & Rössler, W. (2010). Parallel olfactory systems in insects: Anatomy and function. *Annual Review of Entomology*, *55*, 399–420. https://doi.org/10.1146/annurev-ento-112408-085442

Hamanaka, Y., Minoura, R., Nishino, H., Miura, T., & Mizunami, M. (2016). Dopamine- and tyrosine hydroxylase-immunoreactive neurons in the brain of the American cockroach, *Periplaneta americana*. *PLoS One*, *11*, e0160531. https://doi.org/10.1371/journal.pone.0160531

Hanström, B. (1931). Neue Untersuchungen über Sinnesorgane und Nervensystem der Crustaceen I. *Zeitschrift für Morphologie und Oekologie der Tiere*, *23*, 80–236.

Harzsch, S., Anger, K., & Dawirs, R. R. (1997). Immunocytochemical detection of acetylated α-tubulin and Drosophila synapsin in the embryonic crustacean nervous system. *International Journal of Developmental Biology*, *41*, 477–484.

Harzsch, S., & Hansson, B. S. (2008). Brain architecture in the terrestrial hermit crab *Coenobita clypeatus* (Anomura, Coenobitidae), a crustacean with a good aerial sense of smell. *BMC Neuroscience*, *9*, 58. https://doi.org/10.1186/1471-2202-9-58

Klagges, B. R., Heimbeck, G., Godenschwege, T. A., Hofbauer, A., Pflugfelder, G. O., Reifegerste, R., … Buchner, E. (1996). Invertebrate synapsins: A single gene codes for several isoforms in *Drosophila*. *The Journal of Neuroscience*, *16*, 3154–3165.

Krieger, J., Braun, P., Rivera, N. T., Schubart, C. D., Müller, C. H. G., & Harzsch, S. (2015). Comparative analyses of olfactory systems in terrestrial crabs (Brachyura): Evidence for aerial olfaction? *PeerJ*, *3*, e1433. https://doi.org/10.7717/peerj.1433

Li, Y.-S., & Strausfeld, N. J. (1997). Morphology and sensory modality of mushroom body extrinsic neurons in the brain of the cockroach, *Periplaneta americana*. *Journal of Comparative Neurology*, *387*, 631–650. https://doi.org/10.1002/(SICI)1096-9861(19971103)387:4<631::AID-CNE9>3.0.CO;2-3

Lin, C., & Strausfeld, N. J. (2012). Visual inputs to the mushroom body calyces of the whirligig beetle *Dineutus sublineatus*: Modality switching in an insect. *Journal of Comparative Neurology*, *520*, 2562–2574. https://doi.org/10.1002/cne.23092

Marshall, N. J. (1988). A unique colour and polarization vision system in mantis shrimps. *Nature*, *333*, 557–560. https://doi.org/10.1038/333557a0

Marshall, N. J., Cronin, T. W., & Kleinlogel, S. (2007). Stomatopod eye structure and function: A review. *Arthropod Structure & Development*, *36*, 420–448. https://doi.org/10.1016/j.asd.2007.01.006

Maza, F. J., Sztarker, J., Shkedy, A., Peszano, V. N., Locatelli, F. F., & Delorenzi, A. (2016). Context-dependent memory traces in the crab's mushroom bodies: Functional support for a common origin of high-order memory centers. *Proceedings of the National Academy of Science of the United States of America*, *113*, E7957–E7965. https://doi.org/10.1073/pnas.1612418113

Nässel, D. R. (1988). Serotonin and serotonin-immunoreactive neurons in the nervous system of insects. *Progress in Neurobiology*, *30*, 1–85. https://doi.org/10.1016/0301-0082(88)90002-0

Paulk, A. C., & Gronenberg, W. (2008). Higher order visual input to the mushroom bodies in the bee, *Bombus impatiens*. *Arthropod Structure & Development*, *37*, 443–458. https://doi.org/10.1016/j.asd.2008.03.002

Perez-Orive, J., Mazor, O., Turner, G. C., Cassenaer, S., Wilson, R. I., & Laurent, G. (2002). Oscillations and sparsening of odor representations in the mushroom body. *Science*, *297*, 359–365. https://doi.org/10.1126/science.1070502

Sayre, M. E., & Strausfeld, N. J. (2019). Mushroom bodies in crustaceans: Insect-like organization in the caridean shrimp *Lebbeus groenlandicus*. *Journal of Comparative Neurology*, *2019*, 1–17. https://doi.org/10.1002/cne.24678

Schildberger, K. (1984). Multimodal interneurons in the cricket brain: Properties of identified extrinsic mushroom body cells. *Journal of Comparative Physiology A*, *154*, 71–79. https://doi.org/10.1007/BF00605392

Schindelin, J., Arganda-Carreras, I., Frise, E., Kaynig, V., Longair, M., Pietzsch, T., … Cardona, A. (2012). Fiji: An open-source platform for biological-image analysis. *Nature Methods*, *9*, 676–682. https://doi.org/10.1038/nmeth.2019

Skoulakis, E. M., Kalderon, D., & Davis, R. L. (1993). Preferential expression in mushroom bodies of the catalytic subunit of protein kinase A and its role in learning and memory. *Neuron*, *11*, 197–208. https://doi.org/10.1016/0896-6273(93)90178-T

Stemme, T., Iliffe, T. M., & Bicker, G. (2016). Olfactory pathway in *Xibalbanus tulumensis*: Remipedian hemiellipsoid body as homologue of hexapod mushroom body. *Cell and Tissue Research*, *363*, 635–648.

Stern, M. (2009). The PM1 neurons, movement sensitive centrifugal visual brain neurons in the locust: Anatomy, physiology, and modulation by identified octopaminergic neurons. *Journal of Comparative Physiology A*, *195*, 123–137. https://doi.org/10.1007/s00359-008-0392-5

Strausfeld, N. J. (1976). *Atlas of an insect brain*. Berlin, Heidelberg: Springer Verlag.

Strausfeld, N. J. (2012). *Arthropod brains: Evolution, functional elegance, and historical significance*. Boston, MA: Harvard Belknap Press.

Strausfeld, N. J., & Li, Y. (1999). Organization of olfactory and multimodal afferent neurons supplying the calyx and pedunculus of the cockroach mushroom bodies. *Journal of Comparative Neurology*, *409*, 603–625.

Strausfeld, N. J., & Sayre, M. E. (2019). Mushroom bodies in Reptantia reflect a major transition in crustacean brain evolution. *Journal of Comparative Neurology*, *2019*, 1–22. https://doi.org/10.1002/cne.24752

Strausfeld, N. J., Sinakevitch, I., Brown, S. M., & Farris, S. M. (2009). Ground plan of the insect mushroom body: Functional and evolutionary implications. *Journal of Comparative Neurology*, *513*, 265–291. https://doi.org/10.1002/cne.21948

Strausfeld, N. J., Sinakevitch, I., & Okamura, J.-Y. (2007). Organization of local interneurons in optic glomeruli of the dipterous visual system and comparisons with the antennal lobes. *Developmental Neurobiology*, *67*, 1267–1288.

Thazhath, R., Liu, C., & Gaertig, J. (2002). Polyglycylation domain of β-tubulin maintains axonemal architecture and affects cytokinesis in Tetrahymena. *Nature Cell Biology*, *4*, 256–259. https://doi.org/https://doi.org/10.1038/ncb764

Thoen, H. H., Marshall, J., Wolff, G. H., & Strausfeld, N. J. (2017). Insect-like organization of the stomatopod central complex: Functional and phylogenetic implications. *Frontiers in Behavioral Neuroscience*, *11*, 12. https://doi.org/10.3389/fnbeh.2017.00012

Thoen, H. H., Sayre, M. E., Marshall, J., & Strausfeld, N. J. (2018). Representation of the stomatopod's retinal midband in the optic lobes: Putative neural substrates for integrating chromatic, achromatic and polarization information. *Journal of Comparative Neurology*, *526*, 1148–1165. https://doi.org/10.1002/cne.24398

Thoen, H. H., Strausfeld, N. J., & Marshall, J. (2017). Neural organization of afferent pathways from the stomatopod compound eye. *Journal of Comparative Neurology*, *525*, 3010–3030. https://doi.org/10.1002/cne.24256

Vogt, K., Aso, Y., Hige, T., Knapek, S., Ichinose, T., Friedrich, A. B., … Tanimoto, H. (2016). Direct neural pathways convey distinct visual information to Drosophila mushroom bodies. *eLife*, *5*, e14009. https://doi.org/10.7554/eLife.14009

Wolf, H., & Harzsch, S. (2012). Serotonin-immunoreactive neurons in scorpion pectine neuropils: Similarities to insect and crustacean primary olfactory centres? *Zoology*, *115*, 151–159. https://doi.org/10.1016/j.zool.2011.10.002

Wolfe, J. M., Breinholt, J. W., Crandall, K. A., Lemmon, A. R., Lemmon, E. M., Timm, L. E., … Bracken-Grissom, H. D. (2019). A phylogenomic framework, evolutionary timeline and genomic resources for comparative studies of decapod crustaceans. *Proceedings of the Royal Society London B*, *286*, 20190079. https://doi.org/10.1098/rspb.2019.0079

Wolff, G., Thoen, H. H., Marshall, N. J., Sayre, M. E., & Strausfeld, N. J. (2017). An insect-like mushroom body in a crustacean brain. *eLife*, *6*, e29889. https://doi.org/10.7554/eLife.29889

Wolff, G. H., & Strausfeld, N. J. (2015). Genealogical correspondence of mushroom bodies across invertebrate phyla. *Current Biology*, *25*, 38–44. https://doi.org/10.1016/j.cub.2014.10.049

Yamazaki, Y., Nishikawa, N., & Mizunami, M. (1998). Three classes of GABA-like immunoreactive neurons in the mushroom body of the cockroach. *Brain Research*, *788*, 80–86. https://doi.org/10.1016/S0006-8993(97)01515-1

SUPPORTING INFORMATION

Additional supporting information may be found online in the Supporting Information section at the end of this article.

How to cite this article: Thoen HH, Wolff GH, Marshall J, Sayre ME, Strausfeld NJ. The reniform body: An integrative lateral protocerebral neuropil complex of Eumalacostraca identified in Stomatopoda and Brachyura. *J Comp Neurol*. 2020;528:1079–1094. https://doi.org/10.1002/cne.24788